Detail Mapping of surface rupture of the 1990 Rudbar earthquake using remote-sensing techniques

Aflaki, M. [1], Ghods, A. [2], Ajorlou, N. [3], Mousavi, Z. [1], Hollingsworth, J. [4]

[1]*Assistant professor, Department of Earth Sciences, Institute for Advanced Studies in Basic Sciences, Zanjan, Iran, aflaki@iasbs.ac.ir, z.mousavi@iasbs.ac.ir*
[2]*Professor, Department of Earth Sciences, Institute for Advanced Studies in Basic Sciences, Zanjan, Iran, aghods@iasbs.ac.ir*
[3]*PhD student, Department of Earth Sciences, Institute for Advanced Studies in Basic Sciences, Zanjan, Iran, n.ajorlou@iasbs.ac.ir*
[4]*Assistant Professor, Université Grenoble Alpes, ISTerre, Grenoble, France, james.hollingsworth@univ-grenoble-alpes.fr*

ABSTRACT

The 20 June 1990 Rudbar earthquake, M_w 7.3, occurred within a rugged mountainous region causing ~80 km long surface rupture along the Rudbar fault. The earthquake occurred on a NW-striking (~N290º-300º) fault plane with nearly pure sinistral kinematic but shows a complex surface deformation along Zard-Goli and Kabateh segments with reports of normal and reverse movement components. To find how the pure sinistral mechanism at depth could produce the complex surface deformation, we calculate the state of present-day stress by inversion of earthquake's focal mechanisms and also do detail mapping of the earthquake surface rupture using Google Earth images and Optical Image Correlation derived deformation maps. The stress inversion suggests an axis of horizontal maximum stress within N248º-N260º. Our new detailed map of the surface rupture reveals that the rupture along the Zard-Goli and Kabateh segments dominantly include array of minor right stepping en-echelon faults (N260º to N295º striking). It indicates that the orientations of the ruptures are partially parallel to the direction of maximum principal stress, thus resulting in the development of true normal movement component at the surface.

Keywords: Rudbar earthquake rupture, Stress inversion, Remote-sensing, Strike-slip fault.

INTRODUCTION

Present-day deformation of NW Iran is strongly affected by Arabian-Eurasian convergence as well as rigid South Caspian block as a back stop (Ghods et al., 2015). They result in oblique compression along western Alborz and escape of crustal material along NNE- and NW-striking strike-slip faults in NW of Iran and Turkey (e.g. Vernant et al., 2004; Reilinger et al., 2006; Djamour et al., 2011). Along the W. Alborz Mountains, geodetic and geophysical data indicate NE direction of maximum horizontal compression (Vernant et al., 2004; Masson et al., 2014; Zarifi et al., 2014). This can explain for the occurrence of compressional and sinistral strike-slip movements along NW-striking faults (Fig. 1A). However, the 20 June 1990 Rudbar earthquake, M_w 7.3, (Fig. 1B) is known as the first sign of active sinistral kinematic along such a NW-striking fault within the area (Berberian et al., 1992). The event resulted in an ~80 km length surface rupture including three individual Baklor, Kabateh and Zard-Goli segments (Fig. 1B) oriented in a right-stepping en-echelon array (Berberian et al., 1992). Epicenter of the relocated mainshock, and large aftertshocks mostly lies at the central (Kabateh) segment and dominantly concentrate along the NE side of the earthquake surface rupture (Jozi, 2014). Focal mechanism of the mainshock present nearly pure sinistral movement along a NW-striking fault plane (288/88, R -9: Gao et al., 1991; 292/88, R -9: Berberian et al., 1992; 300/75, R -15: Campos et al., 1994), while the larger magnitude aftershocks reveal variety of sinistral to reverse sinistral kinematics along NW-striking faults and reverse kinematic along nearly N-striking faults (Fig. 1B).

The total length of the Rudbar surface rupture was first mapped by Berberian et al. (1992) and

improved during next studies based on field measurements (Berberian and Walker, 2010; Koohpeyma et al., in press) and Optical Image Correlation (OIC) method (Fig. 1C; Ajorlou et al., in preparation). However, there is not yet any detailed mapping of the surface rupture due to either dense vegetation or lack of accessibility to the high mountainous area. Primary reports of the surface ruptures and related displacements indicate SW-dipping high-angle sinistral fault planes at all segments but with a significant reverse displacement component at the Zard-Goli and Kabateh segments (Berberian et al., 1992; Tatar and Hatzfeld, 2009; Berberian and Walker, 2010). New recent field investigations (Koohpeyma et al., in press) present kinematic evidences for NE-dipping fault planes with small normal movement component along Zard-Goli and Kabateh segments. To find how the deep earthquake kinematic is related to the observed surface deformation, we compare the principal axis of stress with the detail map of the surface rupture.

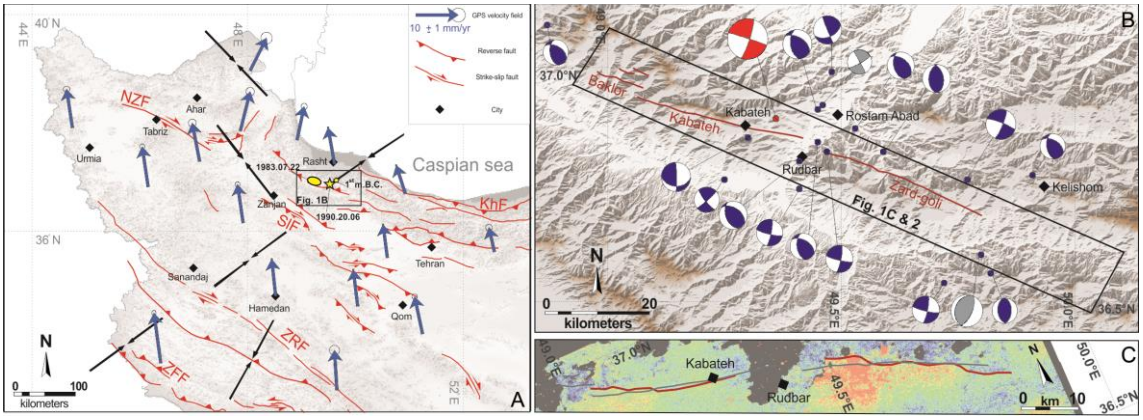

Figure 1. A) Major structural features of NW Iran together with GPS velocity field (blue vectors) from Khorrami et al. (2019) and maximum horizontal stress (black double vectors) from Zarifi et al. (2014) as well as epicenter of 20 Jun 1990 Rudbar mainshock (yellow star) from Jozi (2014) are mapped on DEM (SRTM 90m). Yellow ellipse and pentagon are the mesoseismal area of the 22 July 1983 (M_b 5.6) and the location of the historical earthquake at the 1st millennium B.C., respectively (Berberian et al., 1992). Faults are from Hessami et al. (2003). B) Main segments of Rudbar earthquake surface rupture from Berberian et al. (1992) together with focal mechanism of the mainshock (red beach ball) and major aftershocks (Berberian et al., 1992; Gao and Wallace, 1995) relocated by Jozi (2014). C) The surface rupture (red line) obtained using E-W displacement map deduced from OIC method (Ajorlou, et al., in preparation) is compared with previous one (gray line) from Berberian et al. (1992).

METHODOLOGY

In this research we map in detail the visible parts of the Rudbar earthquake surface rupture using Google Earth imagery and aerial photos. To investigate the relationship between the surface rupture with the mostly sinistral rupture at depth, we estimate the state of present-day stress within the study area. We apply inversion method proposed by Carey-Gailhardis and Mercier (1987) on focal mechanisms of those earthquakes (Fig. 1B) reported by (Berberian et al., 1992; Gao and Wallace, 1995; Jackson et al., 2002) Global CMT solution (https://www.globalcmt.org) and ZUR_RMT (http://www.isc.ac.uk/cgi-bin/agency-get?agency=ZUR_RMT). They include $M_w \geq 4.4$ earthquakes occurred from 1990 to 2012 within the area which are relocated by Jozi (2014). The NW-striking fault plane of the 20 Jun 1990 Rudbar mainshock is used as a key data during the inversion process.

CONCLUSION

We invert the focal mechanism solution of 16 earthquakes (red and blue beach balls in Figure 1B) within the area from 1990 to 2012 ($4.4 \leq M_w \leq 7.3$) to calculate the state of stress in the region. The results indicate an ENE-WNW (N248º to N264º) direction of maximum horizontal compression (Fig. 2A). On the other hand, our detailed mapping of the earthquake surface rupture

(Fig. 2B) reveals a dominant right stepping en-echelon array of minor faults (oriented N260º to N295º) along Kabateh and Zard-Goli segments (Fig. 2C & D). This observation indicates that the earthquake surface ruptures are in some parts parallel to the N288º-N300º striking deep earthquake fault plane (Bernerian et al., 1992; Campos et al., 1994; Gao and Wallace, 1995), but in the other parts oriented in the direction of maximum horizontal compression, thus allowing for development of true normal movement component at the surface such as those reported by Koohpeyma et al. (in press).

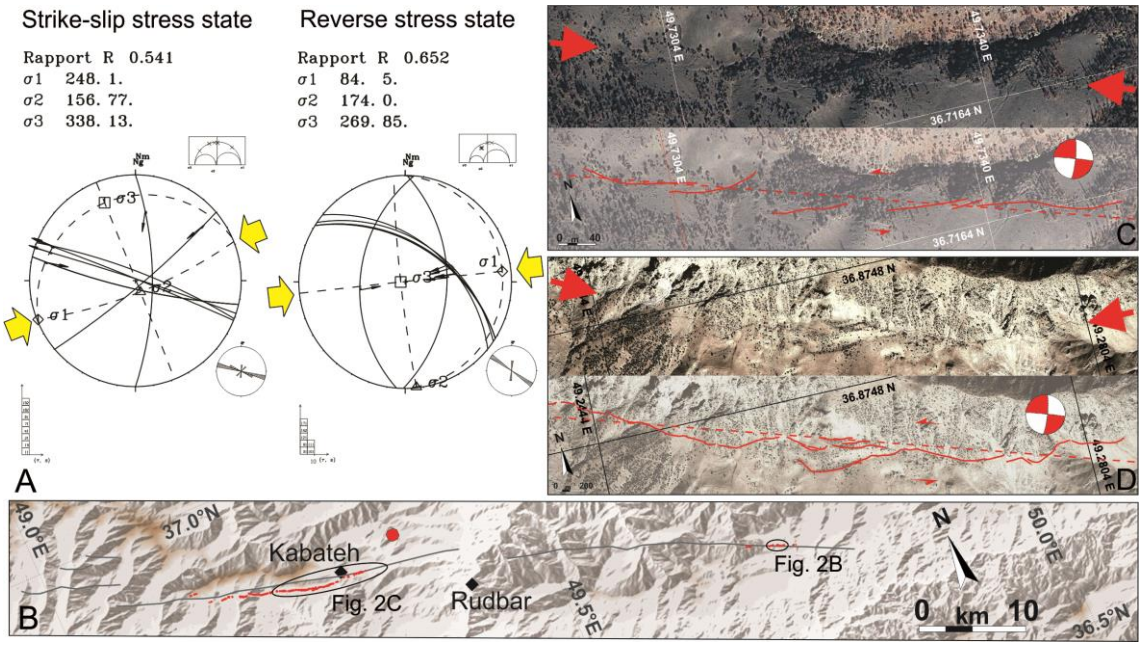

Figure 2. A) States of reverse and strike-slip stress deduced from inversion focal mechanism at Figure 2B (red and blue beach balls). B) Earthquake surface rupture and active faults (red and orange lines, respectively) from this study. Blue and purple lines, respectively, are pre- and post-earthquake landslide areas. Blue triangles are lakes formed by post-earthquake landslides. C & D) Detailed mapping of the earthquake surface rupture at two localities (ellipses on Figure 2D) dominantly reveals right stepping en-echelon array (solid red lines) with respect to the strike of faulting deduced from focal mechanism (red dashed line). The beach ball is the focal mechanism of the mainshock (Berberian et al. 1992).

REFERENCES

-Ajorlou, N., Hollingsworth, J., Mousavi, Z., Ghods, A., Masoumi, Z., in preparation. Characterizing surface deformation in the 1990 Rudbar earthquake (Iran) using optical image processing.

-Berberian, M., Qorashi, M., Jackson, J.A., Priestley, K. and Wallace, T., 1992. The Rudbar-Tarom earthquake of 20 June 1990 in NW Persia: preliminary field and seismological observations, and its tectonic significance. Bulletin of the Seismological Society of America, 82(4), pp.1726-1755.

-Berberian, M. and Walker, R., 2010. The Rudbār M w 7.3 earthquake of 1990 June 20; seismotectonics, coseismic and geomorphic displacements, and historic earthquakes of the western 'High-Alborz', Iran. Geophysical Journal International, 182(3), pp.1577-1602.

-Campos, J., Madariaga, R., Nábělek, J., Bukchin, B.G. and Deschamps, A., 1994. Faulting process of the 1990 June 20 Iran earthquake from broadband records. Geophysical Journal International, 118(1), pp.31-46.

-Carey-Gailhardis, E., Mercier, J.-L., 1987. A numerical method for determining the state of stress using focal mechanism of earthquake populations: application to Tibetan teleseisms and microseismicity of southern Peru. Earth Planet. Sci. Lett. 82, 165–179.

-Djamour et al., 2011 Djamour, Y., Vernant, P., Bayer, R., Nankali, H.R., Ritz, J.F., Hinderer, J., Hatam, Y., Luck, B., Le Moigne, N., Sedighi, M. & Khorrami, F., 2010. GPS and gravity

constraints on continental deformation in the Alborz mountain range, Iran. Geophysical Journal International, 183(3), pp.1287-1301.
-Gao, L. and Wallace, T.C., Jackson, J., 1991. Aftershocks of the June 1990 Rudbar-Tarom earthquake: evidence for slip partitioning. Eos Trans, AGU, 72 (44). Fall Meeting suppl. 335.
-Gao, L. and Wallace, T.C., 1995. The 1990 Rudbar-Tarom Iranian earthquake sequence: Evidence for slip partitioning. Journal of Geophysical Research: Solid Earth, 100(B8), pp.15317-15332.
-Ghods, A., Shabanian, E., Bergman, E., Faridi, M., Donner, S., Mortezanejad, G. & Aziz-Zanjani, A., 2015. The Varzaghan–Ahar, Iran, Earthquake Doublet (M w 6.4, 6.2): implications for the geodynamics of northwest Iran. Geophysical Journal International, 203(1), pp.522-540.
-Hessami, K., Jamali, F. and Tabassi, H., 2003. Major active faults of Iran: Tehran. Iran, International Institute of Earthquake Engineering and Seismology, 1.
-Jackson, J., Priestley, K., Allen, M. and Berberian, M., 2002. Active tectonics of the south Caspian basin. Geophysical Journal International, 148(2), pp.214-245.
-Jozi, 2014, Seismotectonic of northern Iran using local seismic network (M.S. theses, Institute for advanced studies in basic science).
-Khorrami, F., Vernant, P., Masson, F., Nilfouroushan, F., Mousavi, Z., Nankali, H., Saadat, S.A., Walpersdorf, A., Hosseini, S., Tavakoli, P. and Aghamohammadi, A., 2019. An up-to-date crustal deformation map of Iran using integrated campaign-mode and permanent GPS velocities. Geophysical Journal International, 217(2), pp.832-843.
-Kuhpyma, M., Talebian, M., Ghods, A., Nazari, H., Ghoreishi, M., Seismotectonic of the Rudbar-Tarom zone based on temporary (local) seismic network data, Geoscience, in press.
- Masson, F., Lehujeur, M., Ziegler, Y. and Doubre, C., 2014. Strain rate tensor in Iran from a new GPS velocity field. Geophysical Journal International, 197(1), pp.10-21.
-Reilinger, R., McClusky, S., Vernant, P., Lawrence, S., Ergintav, S., Cakmak, R., Ozener, H., Kadirov, F., Guliev, I., Stepanyan, R. & Nadariya, M., 2006. GPS constraints on continental deformation in the Africa-Arabia-Eurasia continental collision zone and implications for the dynamics of plate interactions. Journal of Geophysical Research 111: B05411.
-Tatar, M. and Hatzfeld, D., 2009. Microseismic evidence of slip partitioning for the Rudbar-Tarom earthquake (Ms 7.7) of 1990 June 20 in NW Iran. Geophysical Journal International, 176(2), pp.529-541.
-Vernant, P., Nilforoushan, F., Hatzfeld, D., Abbassi, M.R., Vigny, C., Masson, F., Nankali, H., Martinod, J., Ashtiani, A., Bayer, R., Tavakoli, F. & Chéry, J., 2004. Present-day crustal deformation and plate kinematics in the Middle East constrained by GPS measurements in Iran and northern Oman. Geophys. J. Int. 157 (1), 381–398.